Multimedia Tools and Applications (2019) 78:20431–20463
https://doi.org/10.1007/s11042-019-7383-0

Optimally sectioned and successively reconstructed histogram sub-equalization based gamma correction for satellite image enhancement

Himanshu Singh[1] · **Anil Kumar**[1] · **L. K. Balyan**[1] · **H. N. Lee**[2]

Received: 3 May 2018 / Revised: 16 January 2019 / Accepted: 18 February 2019 /
Published online: 1 March 2019

Abstract
This paper presents an overall quality enhancement approach especially for dark or poorly illuminated images with a core objective to re-allocate the processed pixels using recursive histogram sub-division. An information preserved and image content based behavioral reconstruction inspired adaptive stopping criterion based on pixel-wise relative L_{2}–norm basis (which itself is intuitively related to optimal PSNR value) is proposed in this paper, so that highly adaptive gamma value-set can be derived out of it for sufficient enhancement. Due to this adaptive behavior of the intensity distribution the gamma value-set when derived from it, is obviously highly adaptive and here individual gamma values are evaluated explicitly raised over reconstructed intensity values, unlike conventional gamma correction methods. This adaptiveness makes the entire methodology highly capable for covering a wide variety of images, due to which robustness of the algorithm also increases. The proposed methodology has been verified on various dark images. The simulation results authenticate the overall enhancement (contrast as well as entropy enhancement along with sharpness enhancement) achieved by the proposed has been found superior to other dark image enhancement techniques.

Keywords Sub-histograms, Gamma Correction · Image quality enhancement · Adaptive thresholding, Peak signal to noise ratio (PSNR)

✉ Himanshu Singh
himanshu.iiitj@gmail.com

Anil Kumar
anilkdee@gmail.com

L. K. Balyan
lokendra.balyan@gmail.com

H. N. Lee
heungno@gist.ac.kr

Extended author information available on the last page of the article

1 Introduction

Remotely acquired digital imagery in diverse circumstances and its indispensable contribution for social welfare, demands an efficient quality enhancement as a core part of image pre-processing. In this manner, the required information can be restored and required parametric features can be sufficiently extracted according to the demand [21]. Researchers get highly fascinated by histogram equalization (HE) [5] and its efficiently modified variations due to their simplicity and less computational complexity. Obviously, the global HE cannot preserve local spatial features of the image which limits the amount of quality enhancement in all parts of the image and hence, researchers started looking for distributing histogram into its constituting sub-histograms for local histogram modifications [8, 15, 17, 18]. Fuzzy inspired histogram smoothening followed by local maxima based sub-division has been also proposed as Brightness preserving dynamic fuzzy HE (BPDFHE) [15]. Exposure-based sub-image HE (ESIHE) [17] has been proposed for low exposure images, where image exposure is utilized for sub-division. Afterward, median-mean dependent sub-image-clipped HE (MMSICHE) [18] has been introduced where histogram clipping is based on the median with bisecting each section to obtain four sub-images, so that they can be equalized locally. Later, recursive-ESIHE (R-ESIHE) [19] by iterative usage of ESIHE till exposure reduced to a predefined threshold. Also, its multi-level histogram separation version termed as recursively separated-ESIHE (RS-ESIHE) [19] has been also introduced. Later on, the averaging histogram equalization (AVGHEQ) [11], HE based optimal profile compression (HEOPC) [30] method for color image enhancement followed by HE with maximum intensity coverage (MAXCOVER) [31] have been also proposed. Also, the adaptive gamma correction with weighting distribution (AGCWD) [7] and its efficient variations [16, 20, 24–31] have been also proposed for dark images. Afterward, the intensity and edge-based adaptive unsharp masking filter (IEAUMF) [10] based enhancement have been also proposed by employing the unsharp masking filter for edge augmentation. Sigmoid mapping through cosine transformed Regularized-HE [4] has been also proposed. Recently, getting fascinated by artificial intelligence and deep learning based methods, various methodologies have been also proposed namely, LIME: Low-light image enhancement via illumination map estimation (LIME) [6], Deep photo enhancer: Unpaired learning for image enhancement from photographs with gans (DPE) [3], Learning to See in the Dark (LSD) [2], and Learning a deep single image contrast enhancer from multi-exposure images (LDSICEM) [1]. In the same sequence, although several kinds of enhancement methodologies have been proposed till date for widely diverse characteristics of images from various domains, (contextual literature survey is explicitly presented in [21, 24, 25]), still most of them are lagging when it comes to the matter of enhancement of different domain images through a single approach. In this paper, a robust and highly adaptive end-to-end framework is proposed for quality enhancement of almost all kind of images. On the first sight, the term “gamma correction” seems somehow conventional; but any approach which is capable for computing the quality enhanced intensity distribution out of the input intensity distribution through raising radical powers comes under the head of the gamma correction. Decision making of adaptive gamma value-set precisely for each individual intensity level of the image, is still an open problem, as most of the proposed gamma based (radically powered) algorithms lead to over-enhancement and extreme ends’ saturation, and hereby proposed algorithm seems free from these drawbacks due to deciding a novel kind of gamma value set through “optimal PSNR based perfectly re-allocated and reconstructed” intensity distribution. Here, as such no greedy behavior based optimization algorithm is involved for a blind random search, and hence, the approach is not iterative as a whole. It needs only 2–4 iterations at most for thresholds identification and subsequent histogram division based on optimal PSNR value, but gamma value-set evaluation non-iterative at all. Here, a precisely re-allocated intensity-span is derived through reconstruction of the image by considering first and second moment for histogram sub-division, and later the cumulative distribution of the reconstructed images itself is utilized for deriving a gamma value set. The corresponding individual values from this set when raised up as radicals over the reconstructed and re-allocated intensity levels of the image under consideration leads to the overall quality enhancement. Remaining manuscript is drafted as follows: after brief literature survey and basic introduction in section 1; section 2 explains the proposed algorithm followed by its stepwise framework. Later, section 3 deals with the experimentation followed by corresponding results and discussion; and in section 4, conclusions are drawn.

2 Proposed methodology

Hue-Saturation-Intensity (HSI) colour image model is generally utilized for separation of chromatic as well as non-chromatic image information. For the proposed quality enhancement for the colour images, hue and saturation channels can be kept unaltered along with relevant processing over intensity channel. The entire methodology using process-flow diagram is presented in Fig. 1, and the corresponding step-wise procedure is as follows:

Step 1: Initially, all three channels (R, G, B) are linearly stretched for dynamic range expansion. For R-channel:

$$R(u,v) \leftarrow \frac{R(u,v) - R_{\min}}{R_{\max} - R_{\min}} \tag{1}$$

Here, $R_{max} = max\ \{R(u,v)\}$ and $R_{min} = min\ \{R(u,v)\}$ for all the pixel elements (u,v) for R-channel. Similarly, other two channels can be stretched.

Step 2: Extraction of intensity (luminance or V-channel) information after RGB to HSI colour space conversion as:

$$[H(u,v), S(u,v), I(u,v)]^T = T_{RGB}^{HSI}[R(u,v), G(u,v), B(u,v)]^T, \tag{2}$$

Here, T_{RGB}^{HSI} is RGB to HSI transformation process.

Step 3: Histogram $\{H(h)\}$ of the luminance channel is employed for further processing. Here, $H(h)$ is count of pixels having h^{th} intensity value. Set $a \leftarrow \min(h)$ and $b \leftarrow \max(h)$ which also represents the entire range of histogram starting from its lowest pixel intensity value to largest pixel intensity value. Calculate the mean (μ) and standard deviation (σ) for this operational range $[a, b]$ of the histogram /sub-histogram (for next level division), using:

$$\mu = \frac{\sum_{h=a}^{b} hH(h)}{\sum_{h=a}^{b} H(h)}, \tag{3}$$

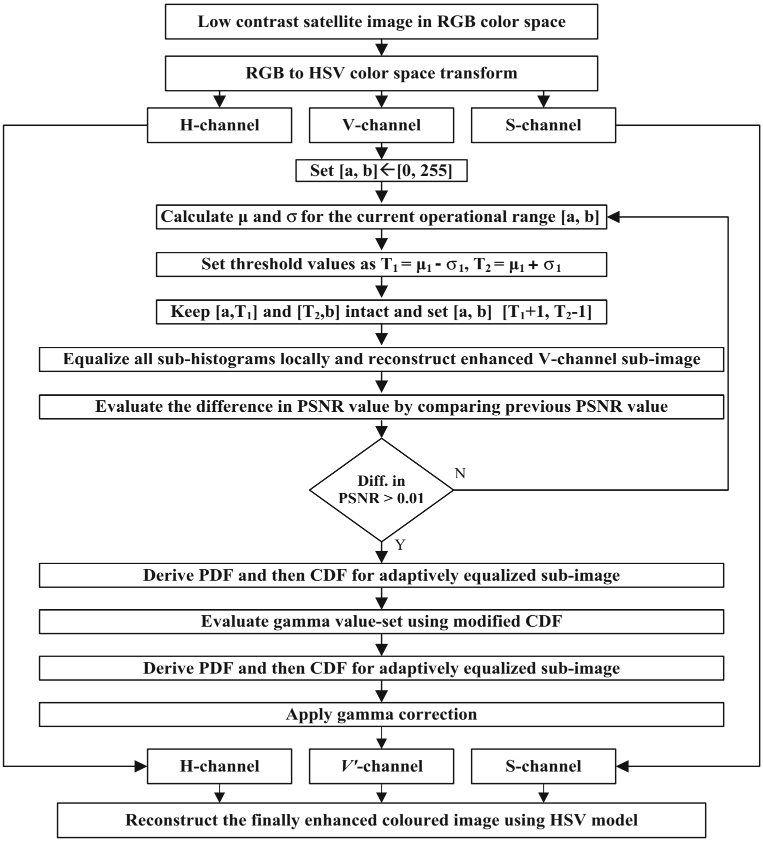

Fig. 1 Process Flow for the proposed methodology

$$\sigma = \left(\frac{\sum_{h=a}^{b}(h-\mu)^2 H(h)}{\sum_{h=a}^{b} H(h)}\right)^{1/2}, \tag{4}$$

Step 4: Set two threshold values i.e. $T_1 = \mu - \sigma$ and $T_2 = \mu + \sigma$, so that the "the operational region" (mentioned in Step 3) can be distributed into its further sub-regions.

Step 5: Store $[a, T_1]$ and $[T_2, b]$ as two parts of the histogram without further distributing them so that they can be retained as such till their equalization in subsequent steps. Consider $[T_1 + 1, T_2 - 1]$ as sub-histogram region $H_k(h)$ so that operations can perform the next step so that it can be adaptively distributed in further recursive steps.

Step 6: Cumulative distribution function (CDF) for each k^{th} sub-histogram can be evaluated as:

$$cdf_k(h) = \frac{1}{N_k} \sum_{h_k+1}^{\mathrm{h}_{k+1}} H_k(h), \tag{5}$$

Here, intensity span of every k^{th} histogram can be considered in the range $[h_k + 1 \rightarrow \mathrm{h}_{k+1}]$. Here, N_k is the net pixel count ink^{th}sub-histogram.

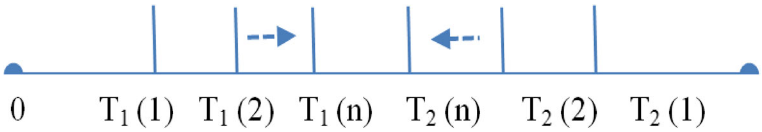

Fig. 2 Multilevel thresholding of intensity value axis

Step 7: Equalize all sub-histograms independently as:

$$\hat{I}_k = I_{k\_\min} + (I_{k\_\max} - I_{k\_\min}) * cdf_k(h), \tag{6}$$

Step 8: Overall reconstructed image can be derived as:

$$\hat{I} = \hat{I}_1 \cup \hat{I}_2 \cup \hat{I}_3 \cup \ldots \cup \hat{I}_k; \tag{7}$$

Step 9: Calculate the value of *PSNR* in dB for enhanced intensity channel obtained in this iteration with reference to that in previous iteration as [31]:

$$PSNR = 10\log_{10}\frac{255}{MSE}, \tag{8}$$

Here, RSME is root-mean-square error, defined as [31]:

$$MSE = \frac{1}{M \times N}\left\|\hat{I} - I\right\|_2^2, \tag{9}$$

Here, I and $\hat{I}$ are input and output images for every iteration. Find the difference of PSNR value obtained in this step with that obtained in the previous step.

Table 1 Number of iterations and corresponding threshold values evaluated for images under consideration

Image S. No.	No. of iterations (i_{max})	Threshold values in lower intensity region $T_1(i)$	Threshold values in higher intensity region $T_2(i)$
1.	2	[21, 37]	[95, 54]
2.	2	[29, 48]	[102, 68]
3.	2	[34, 49]	[99, 73]
4.	2	[19, 42]	[95, 81]
5.	3	[46, 68, 87]	[139, 112, 94]
6.	2	[25, 48]	[98, 75]
7.	2	[33, 51]	[118, 89]
8.	2	[37, 45]	[94, 53]
9.	2	[21, 47]	[85, 61]
10.	2	[31, 48]	[122, 78]
11.	2	[40, 57]	[99, 73]
12.	2	[34, 59]	[126, 93]
13.	2	[32, 49]	[119, 84]
14.	2	[35, 53]	[121, 78]
15.	2	[28, 52]	[117, 81]
16.	3	[68, 84, 102]	[140, 122, 110]
17.	3	[33, 42, 98]	[150, 127, 111]
18.	2	[23, 45]	[95, 81]
19.	2	[31, 48]	[122, 78]
20.	2	[34, 53]	[96, 83]

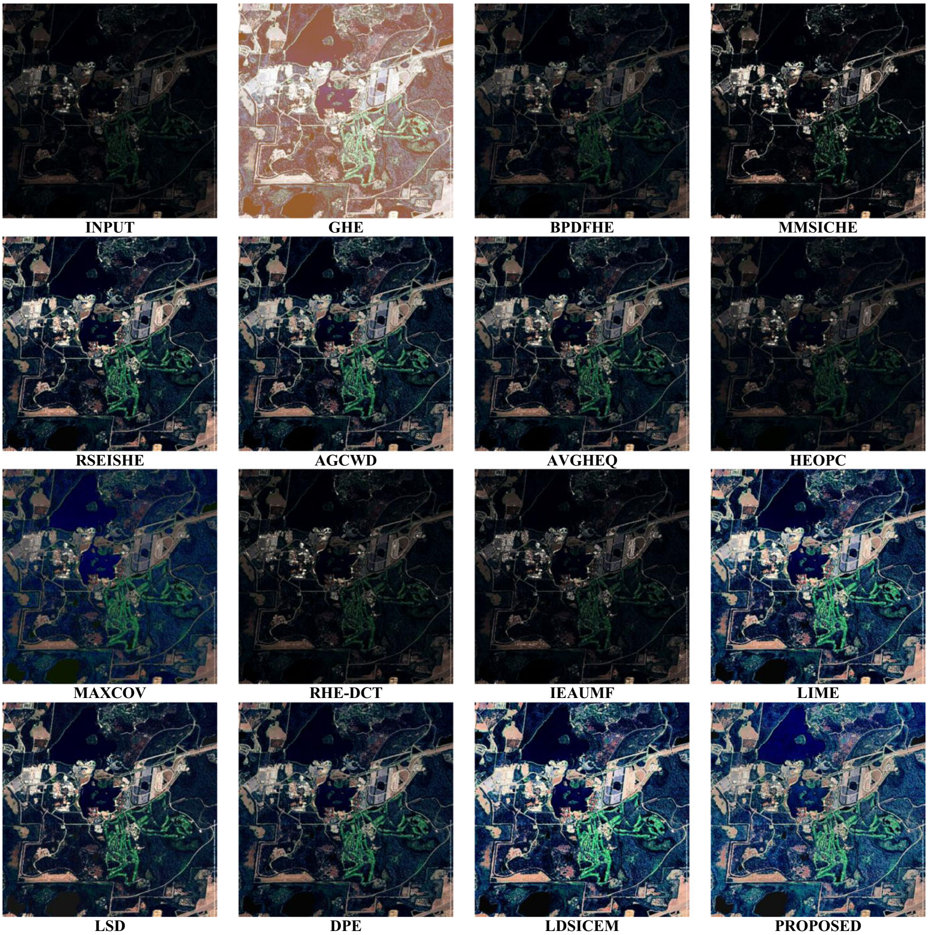

Fig. 3 Quality enhanced results of different algorithms for "Image 1"

Step 10: Now, follow the optimal PSNR criterion to decide the requirement of next level thresholding. Here, recursion is aborted if difference in PSNR values (obtained in successive steps) gets reduced to less than 0.01 dB. In other words, next level thresholding has to be aborted when PSNR value gets saturated, as this saturation symbolizes insignificant further image division/reconstruction; and hence, not appreciated.

Step 11: If the optimal PSNR criterion as mentioned in step-10 is not achieved, then assign $[a, b] \leftarrow [T_1 + 1, T_2 - 1]$ and repeat steps 3–9 for further adaptive separation; and hence, adaptively equalized output can be achieved.

Step 12: Afterwards, cumulative distribution has to be derived reconstructed image so that the adaptive gamma value-set can be derived as:

$$\gamma(i) = 1 - cdf_m(i), \tag{10}$$

Finally, the enhanced output is achieved as:

$$I_{en}(i) = [I(i)]^{\gamma(i)}, \tag{11}$$

Table 2 Brightness (B) values for comparative quantitative evaluation among various algorithms

S.No	INPUT	GHE	BPDFHE	MMSICHE	RSEISHE	AGCWD	AVGHEQ	HEOPC	MAXCOV	RHE-DCT	IEAUMF	LIME	LSD	DPE	LDSICEM	PROPOSED
1	0.071	0.692	0.101	0.125	0.239	0.225	0.178	0.097	0.267	0.094	0.097	0.359	0.270	0.229	0.396	0.436
2	0.181	0.578	0.208	0.230	0.286	0.321	0.229	0.227	0.342	0.236	0.242	0.388	0.421	0.339	0.470	0.377
3	0.257	0.605	0.266	0.295	0.333	0.408	0.319	0.322	0.385	0.344	0.324	0.425	0.454	0.410	0.571	0.474
4	0.145	0.678	0.198	0.175	0.259	0.273	0.194	0.181	0.425	0.185	0.187	0.343	0.383	0.321	0.467	0.406
5	0.352	0.638	0.398	0.379	0.345	0.521	0.637	0.449	0.528	0.455	0.467	0.485	0.510	0.478	0.636	0.599
6	0.316	0.544	0.316	0.350	0.328	0.427	0.394	0.394	0.462	0.403	0.407	0.465	0.450	0.420	0.546	0.454
7	0.127	0.599	0.159	0.178	0.290	0.289	0.244	0.158	0.314	0.165	0.171	0.363	0.424	0.347	0.499	0.431
8	0.297	0.524	0.306	0.331	0.340	0.427	0.386	0.370	0.409	0.388	0.376	0.433	0.470	0.456	0.606	0.469
9	0.175	0.595	0.185	0.210	0.274	0.317	0.218	0.218	0.401	0.226	0.235	0.372	0.396	0.402	0.541	0.424
10	0.313	0.549	0.320	0.347	0.350	0.466	0.396	0.389	0.472	0.402	0.405	0.512	0.474	0.484	0.621	0.497
11	0.235	0.566	0.271	0.279	0.338	0.406	0.292	0.258	0.406	0.311	0.314	0.454	0.457	0.470	0.608	0.466
12	0.235	0.590	0.269	0.277	0.372	0.409	0.319	0.293	0.413	0.328	0.312	0.459	0.490	0.477	0.616	0.473
13	0.569	0.569	0.292	0.320	0.355	0.443	0.365	0.350	0.463	0.356	0.371	0.480	0.437	0.430	0.583	0.502
14	0.552	0.552	0.332	0.356	0.387	0.438	0.462	0.408	0.478	0.410	0.413	0.452	0.470	0.461	0.594	0.468
15	0.586	0.586	0.285	0.287	0.342	0.396	0.343	0.323	0.395	0.328	0.326	0.407	0.448	0.444	0.585	0.451
16	0.631	0.631	0.200	0.223	0.286	0.327	0.237	0.235	0.380	0.238	0.246	0.380	0.407	0.355	0.496	0.406
17	0.608	0.608	0.362	0.404	0.348	0.493	0.542	0.492	0.540	0.491	0.498	0.504	0.460	0.458	0.590	0.528
18	0.570	0.570	0.218	0.252	0.295	0.351	0.292	0.270	0.353	0.280	0.287	0.424	0.465	0.400	0.527	0.435
19	0.623	0.623	0.156	0.219	0.301	0.254	0.375	0.261	0.412	0.269	0.276	0.440	0.381	0.329	0.457	0.386
20	0.695	0.695	0.173	0.231	0.265	0.284	0.293	0.251	0.388	0.260	0.263	0.379	0.397	0.294	0.417	0.359

Table 3 Contrast (V) values for comparative quantitative evaluation among various algorithms

S.No	INPUT	GHE	BPDFHE	MMSICHE	RSEISHE	AGCWD	AVGHEQ	HEOPC	MAXCOV	RHE-DCT	IEAUMF	LIME	LSD	DPE	LDSICEM	PROPOSED
1	0.007	0.018	0.011	0.043	0.057	0.052	0.035	0.009	0.015	0.013	0.017	0.080	0.054	0.041	0.065	0.098
2	0.029	0.056	0.047	0.066	0.071	0.076	0.047	0.044	0.041	0.056	0.065	0.105	0.083	0.082	0.074	0.131
3	0.030	0.052	0.036	0.060	0.049	0.060	0.049	0.046	0.052	0.059	0.050	0.088	0.094	0.062	0.058	0.094
4	0.032	0.024	0.043	0.057	0.069	0.068	0.057	0.049	0.050	0.055	0.057	0.091	0.074	0.074	0.073	0.127
5	0.009	0.061	0.052	0.034	0.024	0.031	0.054	0.018	0.029	0.033	0.057	0.081	0.082	0.053	0.051	0.080
6	0.056	0.072	0.058	0.082	0.067	0.083	0.088	0.085	0.076	0.107	0.114	0.116	0.090	0.091	0.084	0.126
7	0.014	0.047	0.022	0.052	0.062	0.060	0.047	0.021	0.027	0.028	0.032	0.082	0.073	0.066	0.069	0.112
8	0.044	0.080	0.049	0.070	0.058	0.067	0.072	0.067	0.072	0.080	0.085	0.097	0.093	0.068	0.066	0.096
9	0.030	0.048	0.032	0.058	0.065	0.068	0.050	0.047	0.048	0.057	0.064	0.090	0.092	0.083	0.066	0.123
10	0.027	0.071	0.035	0.052	0.041	0.055	0.044	0.042	0.054	0.057	0.074	0.081	0.091	0.077	0.059	0.101
11	0.020	0.070	0.041	0.050	0.052	0.057	0.029	0.023	0.045	0.046	0.055	0.081	0.090	0.078	0.064	0.105
12	0.017	0.052	0.036	0.047	0.047	0.052	0.034	0.026	0.036	0.047	0.054	0.081	0.086	0.076	0.063	0.100
13	0.068	0.068	0.031	0.051	0.052	0.063	0.045	0.040	0.053	0.048	0.082	0.094	0.100	0.068	0.066	0.106
14	0.080	0.080	0.062	0.084	0.087	0.075	0.100	0.095	0.089	0.107	0.099	0.111	0.093	0.085	0.076	0.112
15	0.051	0.051	0.046	0.065	0.067	0.066	0.070	0.063	0.065	0.073	0.068	0.090	0.098	0.078	0.065	0.108
16	0.041	0.041	0.035	0.060	0.066	0.071	0.054	0.049	0.051	0.056	0.064	0.094	0.091	0.078	0.069	0.124
17	0.064	0.064	0.040	0.059	0.046	0.064	0.085	0.066	0.066	0.078	0.105	0.103	0.095	0.087	0.076	0.118
18	0.061	0.061	0.039	0.066	0.066	0.074	0.066	0.053	0.055	0.069	0.078	0.106	0.079	0.088	0.078	0.125
19	0.037	0.037	0.023	0.068	0.080	0.048	0.118	0.056	0.049	0.067	0.081	0.131	0.090	0.078	0.070	0.127
20	0.017	0.017	0.035	0.077	0.079	0.075	0.099	0.068	0.057	0.079	0.093	0.134	0.081	0.080	0.085	0.134

Table 4 Entropy (H) values for comparative quantitative evaluation among various algorithms

S.No	INPUT	GHE	BPDFHE	MMSICHE	RSEISHE	AGCWD	AVGHEQ	HEOPC	MAXCOV	RHE-DCT	IEAUMF	LIME	LSD	DPE	LDSICEM	PROPOSED
1	5.475	3.860	5.216	5.357	5.421	5.405	6.045	5.541	5.780	5.746	5.769	5.422	5.431	6.335	6.142	7.745
2	6.190	5.989	5.788	6.126	6.102	6.021	6.381	6.234	6.318	6.268	6.533	6.097	6.070	6.708	6.340	7.279
3	7.262	6.768	6.902	7.210	7.125	6.968	7.533	7.370	7.648	7.662	7.528	7.159	7.034	7.804	7.383	7.856
4	6.060	4.663	5.720	5.990	5.929	5.830	6.168	6.120	6.359	6.205	6.247	5.944	5.925	6.786	6.460	7.492
5	6.673	7.220	6.495	6.603	6.586	6.549	7.477	7.110	7.430	7.540	7.698	6.566	6.551	7.845	7.438	7.715
6	7.065	6.864	6.671	7.031	7.000	6.637	7.282	7.101	7.182	7.126	7.278	6.939	6.958	7.330	6.845	7.693
7	6.147	5.657	5.905	6.051	6.087	6.034	6.748	6.196	6.553	6.323	6.471	6.078	6.058	7.159	6.820	7.760
8	7.404	7.407	7.026	7.348	7.275	7.024	7.717	7.545	7.696	7.666	7.732	7.270	7.230	7.916	7.438	7.886
9	6.681	5.740	6.315	6.620	6.536	6.433	6.728	6.753	6.912	6.764	6.957	6.567	6.528	7.425	6.995	7.798
10	7.268	6.946	6.894	7.200	7.165	7.003	7.563	7.316	7.691	7.621	7.823	7.165	7.091	7.937	7.411	7.829
11	7.024	6.859	6.695	6.966	6.946	6.855	7.316	7.118	7.580	7.394	7.577	6.949	6.864	7.884	7.366	7.871
12	6.950	6.128	6.701	6.888	6.865	6.795	7.223	7.038	7.398	7.530	7.451	6.854	6.800	7.948	7.412	7.882
13	6.627	6.627	6.539	6.861	6.831	6.734	7.187	6.917	7.347	7.247	7.583	6.833	6.661	7.657	7.261	7.767
14	7.379	7.379	6.891	7.299	7.243	6.808	7.573	7.430	7.494	7.382	7.599	7.202	7.161	7.832	7.287	7.849
15	6.154	6.154	6.767	7.113	6.994	6.814	7.438	7.191	7.473	7.346	7.424	7.049	6.914	7.778	7.281	7.838
16	5.792	5.792	6.057	6.414	6.333	6.227	6.518	6.571	6.667	6.711	6.732	6.358	6.255	7.071	6.694	7.600
17	7.161	7.161	6.621	6.918	6.850	6.728	7.467	7.288	7.348	7.519	7.532	6.863	6.830	7.745	7.237	7.721
18	6.411	6.411	6.381	6.677	6.645	6.496	6.972	6.909	7.001	6.881	7.049	6.599	6.626	7.270	6.806	7.668
19	5.181	5.181	5.608	5.876	5.895	5.727	6.364	6.240	6.296	6.554	6.568	5.816	5.878	6.596	6.258	7.127
20	3.937	3.937	5.341	5.679	5.655	5.465	5.781	5.832	5.769	6.273	5.997	5.544	5.660	6.026	5.731	6.826

Table 5 Sharpness (S) values for comparative quantitative evaluation among various algorithms

S.No	INPUT	GHE	BPDFHE	MMSICHE	RSEISHE	AGCWD	AVGHEQ	HEOPC	MAXCOV	RHE-DCT	IEAUMF	LIME	LSD	DPE	LDSICEM	PROPOSED
1	0.037	0.056	0.053	0.075	0.115	0.115	0.090	0.044	0.074	0.054	0.060	0.156	0.102	0.104	0.176	0.175
2	0.067	0.091	0.082	0.095	0.104	0.108	0.085	0.082	0.079	0.094	0.138	0.128	0.111	0.116	0.145	0.125
3	0.045	0.059	0.049	0.060	0.058	0.064	0.057	0.055	0.061	0.072	0.074	0.076	0.080	0.097	0.124	0.113
4	0.071	0.085	0.099	0.088	0.120	0.130	0.097	0.087	0.095	0.102	0.108	0.152	0.134	0.153	0.208	0.169
5	0.035	0.082	0.082	0.066	0.056	0.063	0.083	0.050	0.063	0.072	0.181	0.102	0.102	0.099	0.118	0.110
6	0.074	0.084	0.076	0.090	0.083	0.090	0.093	0.092	0.087	0.106	0.175	0.106	0.093	0.102	0.117	0.110
7	0.067	0.125	0.086	0.117	0.145	0.146	0.126	0.082	0.098	0.097	0.109	0.172	0.162	0.157	0.206	0.175
8	0.054	0.080	0.059	0.070	0.064	0.069	0.070	0.067	0.071	0.084	0.132	0.081	0.084	0.096	0.114	0.107
9	0.057	0.074	0.059	0.072	0.086	0.093	0.072	0.070	0.080	0.082	0.115	0.107	0.107	0.112	0.136	0.111
10	0.051	0.088	0.057	0.067	0.063	0.072	0.066	0.064	0.073	0.079	0.178	0.088	0.091	0.102	0.115	0.105
11	0.066	0.120	0.092	0.100	0.105	0.110	0.067	0.066	0.083	0.103	0.146	0.131	0.137	0.141	0.160	0.150
12	0.064	0.103	0.092	0.098	0.105	0.112	0.089	0.079	0.098	0.110	0.158	0.139	0.145	0.146	0.167	0.159
13	0.081	0.081	0.044	0.059	0.058	0.060	0.052	0.049	0.058	0.060	0.186	0.077	0.081	0.086	0.104	0.097
14	0.088	0.088	0.072	0.082	0.085	0.083	0.093	0.087	0.086	0.103	0.108	0.098	0.093	0.110	0.126	0.112
15	0.083	0.083	0.078	0.085	0.092	0.095	0.093	0.087	0.091	0.105	0.109	0.109	0.115	0.139	0.164	0.141
16	0.067	0.067	0.058	0.069	0.080	0.086	0.070	0.067	0.069	0.078	0.110	0.098	0.096	0.101	0.129	0.110
17	0.071	0.071	0.056	0.073	0.062	0.060	0.076	0.066	0.067	0.081	0.176	0.090	0.091	0.095	0.100	0.091
18	0.137	0.137	0.101	0.124	0.134	0.149	0.135	0.121	0.122	0.144	0.176	0.178	0.152	0.165	0.199	0.172
19	0.060	0.060	0.046	0.068	0.086	0.071	0.106	0.074	0.068	0.091	0.135	0.118	0.089	0.095	0.123	0.104
20	0.040	0.040	0.057	0.080	0.086	0.088	0.097	0.080	0.073	0.098	0.135	0.117	0.088	0.097	0.123	0.113

Table 6 Colorfulness (C) values for comparative quantitative evaluation among various algorithms

S.No	INPUT	GHE	BPDFHE	MMSICHE	RSEISHE	AGCWD	AVGHEQ	HEOPC	MAXCOV	RHE-DCT	IEAUMF	LIME	LSD	DPE	LDSICEM	PROPOSED
1	0.048	0.921	0.060	0.060	0.132	0.131	0.100	0.055	0.185	0.052	0.051	0.222	0.141	0.285	0.177	0.242
2	0.136	0.289	0.078	0.086	0.108	0.125	0.086	0.085	0.137	0.090	0.096	0.151	0.153	0.369	0.397	0.392
3	0.228	0.474	0.131	0.135	0.166	0.215	0.156	0.160	0.202	0.170	0.159	0.212	0.237	0.337	0.342	0.356
4	0.240	0.180	0.164	0.160	0.210	0.222	0.167	0.152	0.278	0.158	0.162	0.267	0.274	0.521	0.624	0.595
5	0.359	0.592	0.252	0.229	0.211	0.316	0.368	0.269	0.313	0.276	0.295	0.308	0.323	0.811	0.881	0.898
6	0.325	0.249	0.083	0.089	0.084	0.118	0.104	0.103	0.122	0.106	0.114	0.124	0.116	0.380	0.385	0.389
7	0.075	0.408	0.074	0.083	0.139	0.138	0.117	0.075	0.169	0.078	0.080	0.176	0.203	0.304	0.380	0.376
8	0.023	0.240	0.054	0.058	0.059	0.077	0.068	0.064	0.072	0.069	0.067	0.079	0.085	0.204	0.249	0.246
9	0.224	0.292	0.085	0.101	0.125	0.145	0.101	0.101	0.211	0.105	0.107	0.170	0.177	0.327	0.262	0.342
10	0.194	0.337	0.092	0.097	0.103	0.144	0.119	0.118	0.142	0.118	0.127	0.152	0.135	0.546	0.572	0.590
11	0.250	0.341	0.115	0.121	0.143	0.169	0.117	0.109	0.163	0.132	0.132	0.189	0.190	0.550	0.566	0.576
12	0.215	0.342	0.120	0.124	0.171	0.186	0.144	0.134	0.203	0.149	0.144	0.206	0.224	0.538	0.578	0.563
13	0.319	0.319	0.111	0.118	0.133	0.172	0.141	0.135	0.172	0.135	0.141	0.182	0.165	0.544	0.584	0.598
14	0.327	0.327	0.110	0.118	0.128	0.145	0.152	0.134	0.159	0.134	0.136	0.150	0.154	0.465	0.459	0.471
15	0.367	0.367	0.117	0.110	0.138	0.174	0.139	0.129	0.162	0.133	0.132	0.172	0.196	0.539	0.612	0.564
16	0.456	0.456	0.136	0.159	0.194	0.222	0.161	0.160	0.261	0.162	0.168	0.256	0.265	0.537	0.656	0.606
17	0.562	0.562	0.208	0.228	0.199	0.291	0.304	0.278	0.309	0.285	0.288	0.292	0.262	0.564	0.626	0.627
18	0.321	0.321	0.088	0.104	0.119	0.141	0.117	0.109	0.150	0.113	0.117	0.170	0.183	0.489	0.491	0.499
19	0.320	0.320	0.087	0.121	0.166	0.147	0.211	0.134	0.234	0.153	0.150	0.254	0.200	0.121	0.135	0.139
20	0.153	0.153	0.120	0.160	0.183	0.203	0.205	0.166	0.244	0.183	0.186	0.268	0.241	0.599	0.680	0.650

Table 7 GLCM Homogeneity (GH) values for comparative quantitative evaluation among various algorithms

S.No	INPUT	GHE	BPDFHE	MMSICHE	RSEISHE	AGCWD	AVGHEQ	HEOPC	MAXCOV	RHE-DCT	IEAUMF	LIME	LSD	DPE	LDSICEM	PROPOSED
1	0.903	0.759	0.820	0.843	0.641	0.652	0.704	0.863	0.686	0.839	0.833	0.556	0.634	0.644	0.539	0.501
2	0.760	0.687	0.733	0.715	0.677	0.669	0.718	0.721	0.677	0.705	0.629	0.636	0.631	0.650	0.627	0.615
3	0.801	0.758	0.789	0.771	0.757	0.734	0.761	0.762	0.740	0.719	0.713	0.713	0.708	0.635	0.612	0.597
4	0.760	0.712	0.684	0.740	0.629	0.618	0.695	0.715	0.644	0.693	0.687	0.575	0.566	0.558	0.523	0.511
5	0.815	0.674	0.659	0.722	0.730	0.704	0.668	0.753	0.709	0.679	0.522	0.621	0.621	0.605	0.603	0.590
6	0.723	0.693	0.717	0.691	0.703	0.695	0.680	0.681	0.675	0.669	0.552	0.671	0.672	0.651	0.654	0.629
7	0.762	0.602	0.716	0.705	0.590	0.592	0.624	0.713	0.628	0.691	0.673	0.552	0.540	0.562	0.528	0.516
8	0.767	0.696	0.755	0.742	0.742	0.729	0.726	0.732	0.721	0.701	0.607	0.707	0.699	0.641	0.640	0.621
9	0.781	0.701	0.770	0.755	0.701	0.681	0.742	0.743	0.673	0.723	0.673	0.651	0.647	0.627	0.621	0.611
10	0.788	0.698	0.772	0.749	0.757	0.723	0.743	0.747	0.715	0.712	0.524	0.691	0.692	0.651	0.659	0.641
11	0.742	0.633	0.693	0.694	0.659	0.641	0.726	0.734	0.678	0.660	0.596	0.609	0.606	0.583	0.594	0.561
12	0.726	0.648	0.673	0.672	0.634	0.611	0.663	0.690	0.636	0.622	0.565	0.572	0.566	0.554	0.567	0.528
13	0.696	0.696	0.806	0.766	0.769	0.753	0.778	0.788	0.747	0.757	0.544	0.713	0.712	0.672	0.661	0.647
14	0.685	0.685	0.721	0.711	0.705	0.706	0.690	0.701	0.696	0.681	0.652	0.688	0.682	0.628	0.633	0.616
15	0.699	0.699	0.708	0.708	0.677	0.660	0.677	0.690	0.665	0.658	0.642	0.646	0.634	0.569	0.568	0.556
16	0.755	0.755	0.776	0.759	0.724	0.708	0.749	0.753	0.705	0.731	0.686	0.685	0.680	0.663	0.641	0.629
17	0.689	0.689	0.734	0.691	0.723	0.720	0.679	0.703	0.694	0.665	0.538	0.656	0.651	0.632	0.653	0.636
18	0.580	0.580	0.644	0.619	0.578	0.554	0.577	0.597	0.561	0.573	0.538	0.520	0.513	0.522	0.515	0.494
19	0.755	0.755	0.812	0.758	0.695	0.746	0.668	0.723	0.722	0.694	0.627	0.657	0.669	0.670	0.641	0.638
20	0.804	0.804	0.776	0.729	0.708	0.713	0.692	0.714	0.715	0.690	0.646	0.668	0.711	0.676	0.653	0.641

Table 8 GLCM Energy (GE) values for comparative quantitative evaluation among various algorithms

S.No	INPUT	GHE	BPDFHE	MMSICHE	RSEISHE	AGCWD	AVGHEQ	HEOPC	MAXCOV	RHE-DCT	IEAUMF	LIME	LSD	DPE	LDSICEM	PROPOSED
1	0.553	0.210	0.313	0.526	0.091	0.111	0.152	0.434	0.118	0.392	0.425	0.035	0.079	0.083	0.033	0.022
2	0.141	0.081	0.145	0.128	0.081	0.076	0.106	0.107	0.056	0.111	0.101	0.061	0.045	0.070	0.067	0.052
3	0.114	0.073	0.102	0.106	0.074	0.053	0.078	0.078	0.057	0.060	0.070	0.050	0.051	0.037	0.045	0.030
4	0.241	0.161	0.148	0.228	0.084	0.079	0.153	0.173	0.055	0.163	0.166	0.053	0.038	0.051	0.045	0.030
5	0.177	0.051	0.042	0.105	0.080	0.060	0.047	0.098	0.066	0.055	0.032	0.031	0.031	0.032	0.048	0.036
6	0.069	0.055	0.069	0.060	0.065	0.060	0.051	0.050	0.038	0.057	0.045	0.055	0.045	0.046	0.066	0.039
7	0.240	0.055	0.177	0.213	0.053	0.056	0.072	0.149	0.061	0.137	0.139	0.039	0.027	0.039	0.032	0.025
8	0.089	0.040	0.077	0.081	0.067	0.055	0.055	0.060	0.051	0.051	0.045	0.050	0.044	0.032	0.056	0.030
9	0.182	0.084	0.168	0.165	0.090	0.073	0.134	0.131	0.054	0.130	0.126	0.053	0.054	0.041	0.056	0.033
10	0.097	0.053	0.086	0.081	0.076	0.053	0.064	0.066	0.048	0.050	0.027	0.040	0.043	0.033	0.068	0.037
11	0.099	0.039	0.078	0.086	0.051	0.037	0.075	0.088	0.045	0.053	0.053	0.029	0.032	0.026	0.051	0.025
12	0.104	0.064	0.072	0.087	0.047	0.035	0.060	0.076	0.047	0.043	0.061	0.026	0.025	0.023	0.050	0.023
13	0.057	0.057	0.102	0.091	0.080	0.066	0.082	0.089	0.055	0.075	0.040	0.051	0.064	0.042	0.058	0.040
14	0.045	0.045	0.064	0.062	0.054	0.058	0.046	0.054	0.046	0.056	0.048	0.056	0.044	0.033	0.063	0.030
15	0.078	0.078	0.073	0.083	0.055	0.045	0.055	0.061	0.043	0.057	0.056	0.044	0.044	0.027	0.044	0.025
16	0.115	0.115	0.146	0.143	0.088	0.075	0.114	0.114	0.055	0.111	0.107	0.064	0.064	0.060	0.061	0.042
17	0.051	0.051	0.083	0.064	0.077	0.073	0.048	0.058	0.052	0.048	0.031	0.048	0.048	0.041	0.067	0.043
18	0.054	0.054	0.091	0.084	0.053	0.042	0.054	0.060	0.034	0.061	0.059	0.033	0.023	0.031	0.040	0.024
19	0.140	0.140	0.198	0.166	0.092	0.121	0.080	0.104	0.079	0.105	0.099	0.079	0.072	0.080	0.073	0.058
20	0.248	0.248	0.193	0.164	0.137	0.133	0.133	0.138	0.104	0.142	0.139	0.116	0.150	0.119	0.106	0.093

Table 9 GLCM Correlation (GC) values for comparative quantitative evaluation among various algorithms

S.No	INPUT	GHE	BPDFHE	MMSICHE	RSEISHE	AGCWD	AVGHEQ	HEOPC	MAXCOV	RHE-DCT	IEAUMF	LIME	LSD	DPE	LDSICEM	PROPOSED
1	0.516	0.544	0.500	0.534	0.544	0.533	0.550	0.506	0.357	0.480	0.432	0.480	0.540	0.530	0.462	0.284
2	0.575	0.613	0.592	0.587	0.597	0.603	0.586	0.584	0.591	0.573	0.417	0.607	0.610	0.595	0.592	0.529
3	0.802	0.816	0.803	0.805	0.804	0.817	0.811	0.810	0.813	0.770	0.755	0.822	0.819	0.678	0.647	0.601
4	0.663	0.436	0.583	0.652	0.602	0.554	0.647	0.660	0.636	0.604	0.551	0.547	0.546	0.469	0.416	0.388
5	0.656	0.757	0.719	0.682	0.701	0.712	0.724	0.690	0.708	0.663	0.174	0.723	0.724	0.639	0.639	0.570
6	0.662	0.674	0.662	0.666	0.657	0.665	0.667	0.666	0.663	0.653	0.474	0.671	0.670	0.652	0.649	0.600
7	0.357	0.365	0.351	0.342	0.348	0.344	0.351	0.345	0.343	0.320	0.277	0.346	0.348	0.334	0.325	0.277
8	0.801	0.779	0.792	0.792	0.799	0.794	0.803	0.803	0.802	0.761	0.603	0.806	0.794	0.700	0.677	0.644
9	0.679	0.670	0.681	0.691	0.690	0.674	0.692	0.691	0.665	0.659	0.528	0.677	0.672	0.647	0.627	0.602
10	0.714	0.720	0.731	0.736	0.716	0.747	0.727	0.725	0.737	0.712	0.386	0.755	0.758	0.691	0.683	0.613
11	0.561	0.604	0.568	0.547	0.572	0.605	0.653	0.599	0.677	0.550	0.359	0.606	0.607	0.553	0.549	0.447
12	0.535	0.601	0.558	0.548	0.564	0.572	0.562	0.550	0.543	0.546	0.295	0.579	0.575	0.530	0.505	0.405
13	0.761	0.761	0.798	0.782	0.800	0.837	0.814	0.812	0.829	0.787	0.393	0.831	0.820	0.758	0.762	0.723
14	0.722	0.722	0.732	0.740	0.740	0.722	0.738	0.741	0.743	0.699	0.693	0.731	0.727	0.647	0.622	0.606
15	0.710	0.710	0.724	0.715	0.729	0.724	0.726	0.728	0.731	0.675	0.663	0.726	0.724	0.559	0.540	0.501
16	0.679	0.679	0.698	0.707	0.711	0.702	0.709	0.709	0.730	0.664	0.543	0.706	0.702	0.655	0.643	0.600
17	0.760	0.760	0.736	0.710	0.717	0.787	0.779	0.776	0.783	0.732	0.460	0.750	0.730	0.702	0.736	0.712
18	0.417	0.417	0.462	0.471	0.465	0.438	0.463	0.466	0.472	0.417	0.321	0.439	0.442	0.434	0.398	0.366
19	0.721	0.721	0.743	0.794	0.768	0.719	0.753	0.754	0.759	0.698	0.545	0.721	0.758	0.721	0.697	0.659
20	0.658	0.658	0.718	0.742	0.736	0.684	0.722	0.729	0.743	0.670	0.546	0.692	0.706	0.670	0.671	0.630

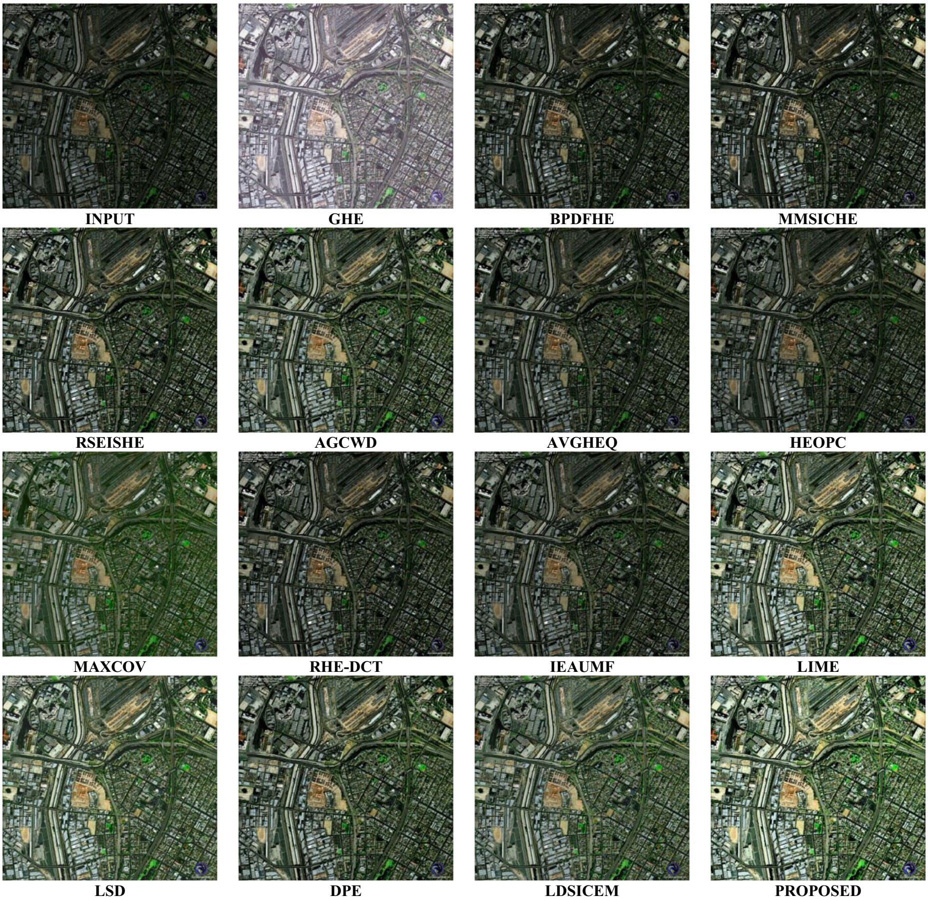

Fig. 4 Quality enhanced results of different algorithms for "Image 2"

Step 13: Finally, the enhanced image can be obtained as:

$$[R(u,v), G(u,v), B(u,v)]^T = T_{HSI}^{RGB}\left[H(u,v), S(u,v), \hat{I}(u,v)\right]^T, \tag{12}$$

Here, T_{HSI}^{RGB} is *HSI* to *RGB* transformation process.

At the first attempt, two (2) threshold values are identified and hence, results into three (3) sub-histograms, followed by their individual equalization. If the stopping criterion will not get satisfied (i.e., PSNR >0.01 dB), then both of the above thresholds will be treated as extreme end of the middle sub-histogram which is further subdivided in the similar fashion as mentioned above. Hence, the new threshold values will be identified in-between the previous threshold values. In this manner, by the end of second attempt of division, there will be four (4) threshold values and accordingly five (5) sub-histograms. In most of these cases, it is insignificant to looking forward for further sub-division.

Fig. 5 Quality enhanced results of different algorithms for "Image 3"

3 Experimental results: performance evaluation and comparisons

Multilevel iterative thresholds are shown in Fig. 2. Table 1 lists the number of iterations and corresponding threshold values evaluated iteratively (as shown in Fig. 3) for all test images. The iteration-count varies adaptively according to the intensity spread of the image. Performance evaluation and comparison is done by proper reimplementation of some very popular state-of-the-art enhancement methodologies namely, GHE [5], BPDFHE [15], MMSICHE [18], RSEISHE [19], AGCWD, AVGHEQ [11], HEOPC [22], MAXCOV [23], RHE-DCT [4], IEAUMF [10], LIME [6], LSD [3], DPE [2] and LDSICEM [1]. Quantitative analysis (Tables 2, 3, 4, 5, 6, 7, 8 and 9) is done by using 8 reliable statistical performance measures namely, average brightness (B), average contrast (V), average discrete information content (or entropy, E), sharpness (S), and colorfulness (C) of the image. Considering intensity value $I(u, v)$ for pixel element located at u^{th} row and v^{th} column of its equivalent image $M \times N$ matrix whose size is similar to that of corresponding intensity channel of the image, and its performance measures can be formulated as follows.

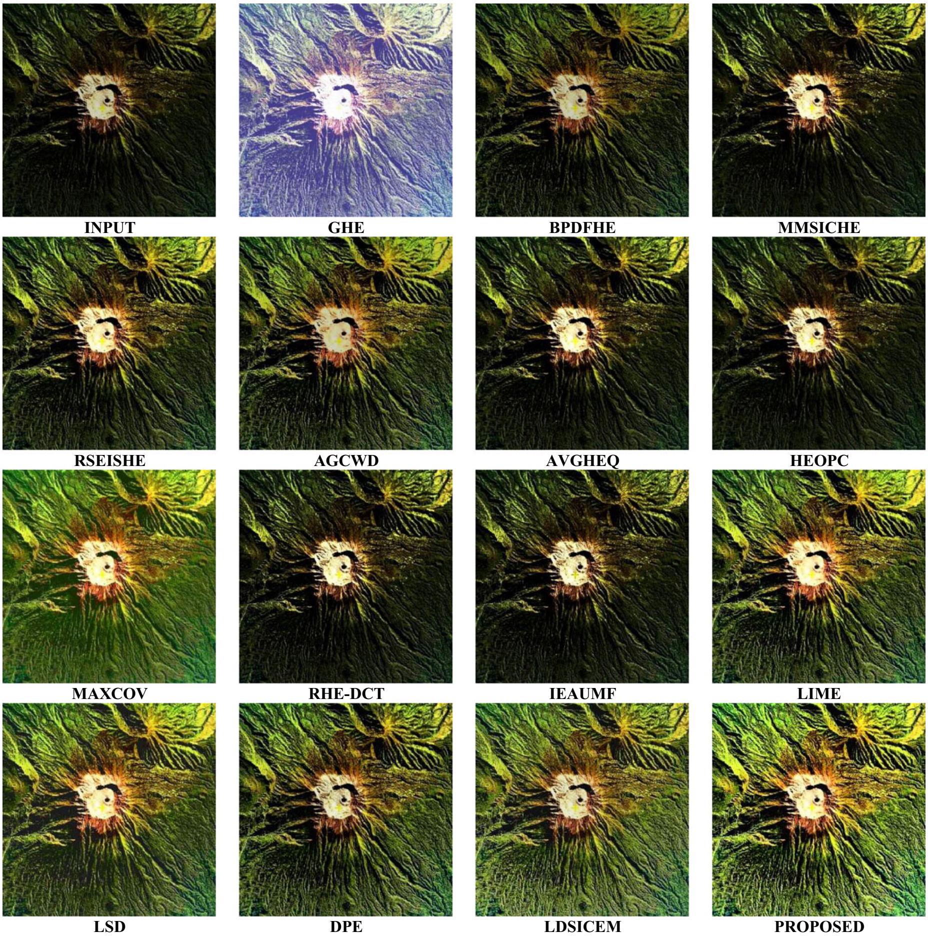

Fig. 6 Quality enhanced results of different algorithms for "Image 4"

Mean represents the average intensity value [11], which indirectly informs about the average image brightness level for the image under consideration. Brightness (B) or mean can be expressed as:

$$B = \frac{1}{M^{*}N} \sum_{u=1}^{M} \sum_{v=1}^{N} I(u, v), \tag{13}$$

Likewise, intensity spread or variance *(V)* or contrast indicates the amount of intensity deviation per pixel with respect to the mean intensity level *(B)* of the image, as:

$$V = \frac{1}{M^{*}N} \sum_{u,v} I(u, v)^{2} - \left(\frac{1}{M^{*}N} \sum_{u,v} I(u, v) \right)^{2}, \tag{14}$$

In this manner, the total sum of the intensity dispersions (w.r.t. mean level) can be identified as contrast and obviously it should be high for proper quality enhancement. In addition, for proper information content evaluation, Shannon entropy based characterization can be applied as:

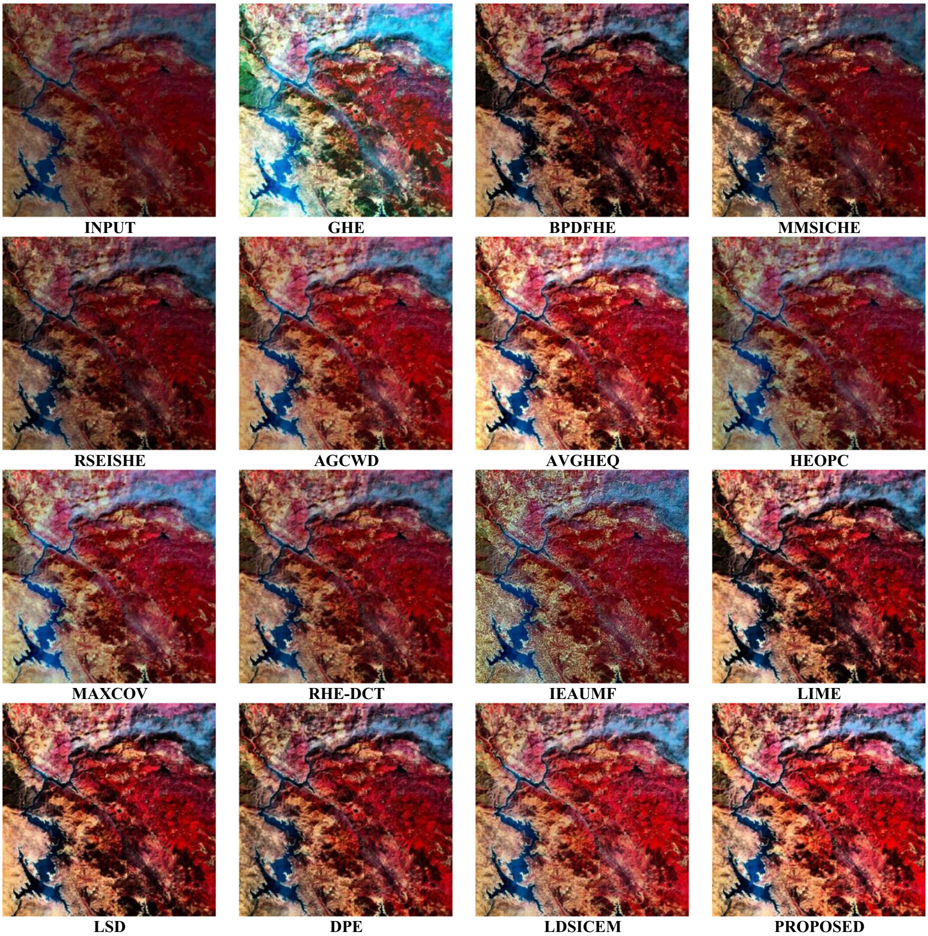

Fig. 7 Quality enhanced results of different algorithms for "Image 5"

$$H = -\sum_{i=0}^{I_{\max}} p_i \log_2(p_i), \tag{15}$$

where, $p_i = n_i/(M \times N)$ is the possibility of existence of i^{th} level of intensity, and $I_{\max}$ is the maximum available intensity. Here, $M \times N$ represents the total number of pixels present in an image. The gradient is obtained from:

$$S = \frac{1}{M^* N} \sum_{u,v} \left(\sqrt{\Delta u^2 + \Delta v^2} \right), \tag{16}$$

$\Delta u = I_{enh}(u, v) - I_{enh}(u+1, v) and$ $\Delta v = I_{enh}(u, v) - I_{enh}(u, v+1)$ are the local gradients of enhanced image. Higher the gradient value more will be the sharpness of image. Along with above intensity based measures, colorfulness is also used for proper evaluation of the quality of color images. The colorfulness can be expressed numerically, as:

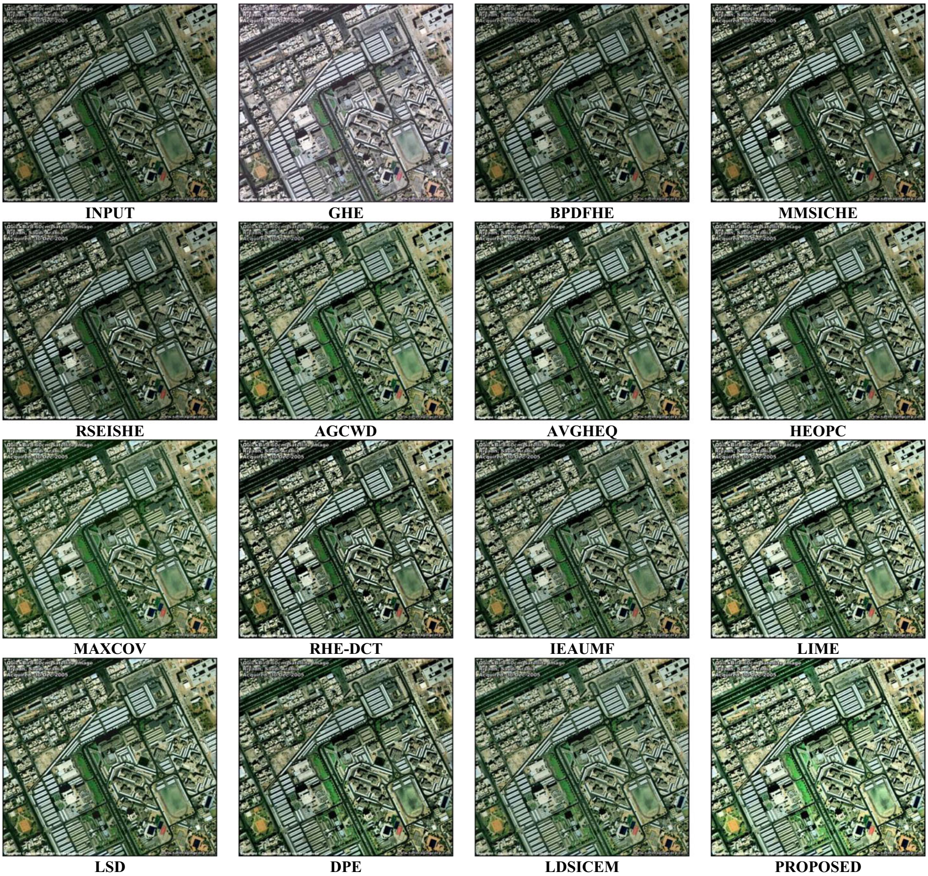

Fig. 8 Quality enhanced results of different algorithms for "Image 6"

$$C = \sqrt{\sigma_{rg}^2 + \sigma_{yb}^2} + 0.3\sqrt{\mu_{rg}^2 + \mu_{yb}^2}, \tag{17}$$

$$\Delta rg = R - G, \tag{18}$$

$$\Delta yb = 0.5(R + G) - B, \tag{19}$$

Here, μ_{rg}, μ_{yb} are the mean values and σ_{rg}, σ_{yb} are the standard deviation values of Δ_{rg}, Δ_{yb} respectively. Spatial co-occurrence of the image pixels are usually avoided while evaluating the intensity based indices, and hence, to resolve it, Grey-Level Co-occurrence Matrix based performance indices also plays a significant role for texture and other spatially influenced properties. Overall statistical and spatial behavior w.r.t. reference pixel can be derived by calculating the pixel-wise average for all four directional matrices:

$$GLCM = 0.25\left(GLCM_0 + GLCM_{\pi/4} + GLCM_{\pi/2} + GLCM_{3\pi/4}\right); \tag{20}$$

In this paper, three well known GLCM based indices, i.e. GLCM-Correlation, GLCM-Energy and GLCM-Homogeneity are evaluated. Any element of the GLCM matrix $\Psi(m, n)$, is usually

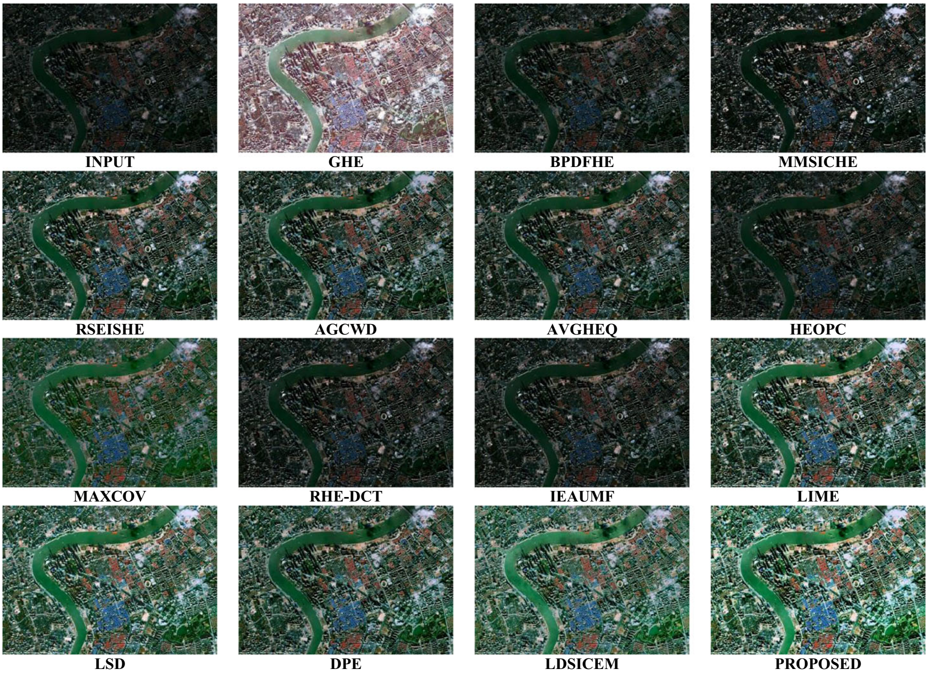

Fig. 9 Quality enhanced results of different algorithms for "Image 7"

evaluated by considering the n^{th} neighboring pixel w.r.t. m^{th} pixel, and later on, by calculating the μ_m, μ_n, σ_m, $and \sigma_n$ as the corresponding mean values and standard deviation values respectively. GLCM-correlation (GC) stands for the interdependency for the corresponding neighborhood of the pixels w.r.t. reference pixels, expressed as:

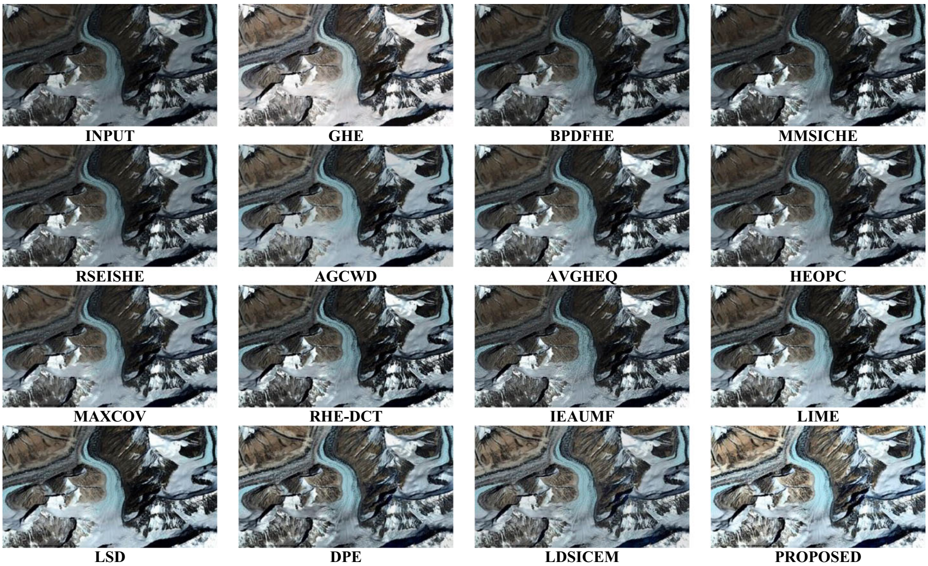

Fig. 10 Quality enhanced results of different algorithms for "Image 8"

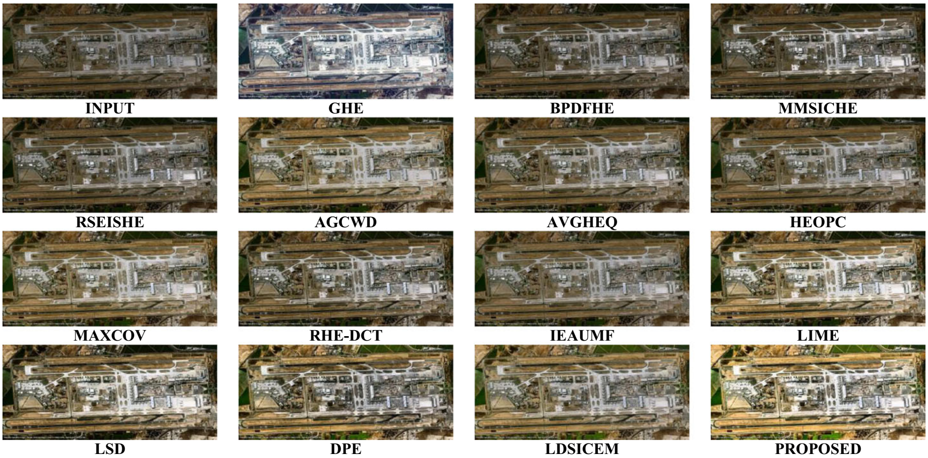

Fig. 11 Quality enhanced results of different algorithms for "Image 9"

$$GC = \sum_{m=0}^{M-1} \sum_{n=0}^{N-1} \frac{(m-\mu_m)(n-\mu_n)\Psi(m,n)}{\sigma_m.\sigma_n}, \tag{21}$$

GLCM-Energy (*GE*) can be characterized by normalized count of repeated pairs. Intuitively, these are responsible for uniformity of texture, and hence, expressed as:

$$GLCM-Energy(GE) = \sum_{m=0}^{M-1} \sum_{n=0}^{N-1} \Psi(m,n)^2, \tag{22}$$

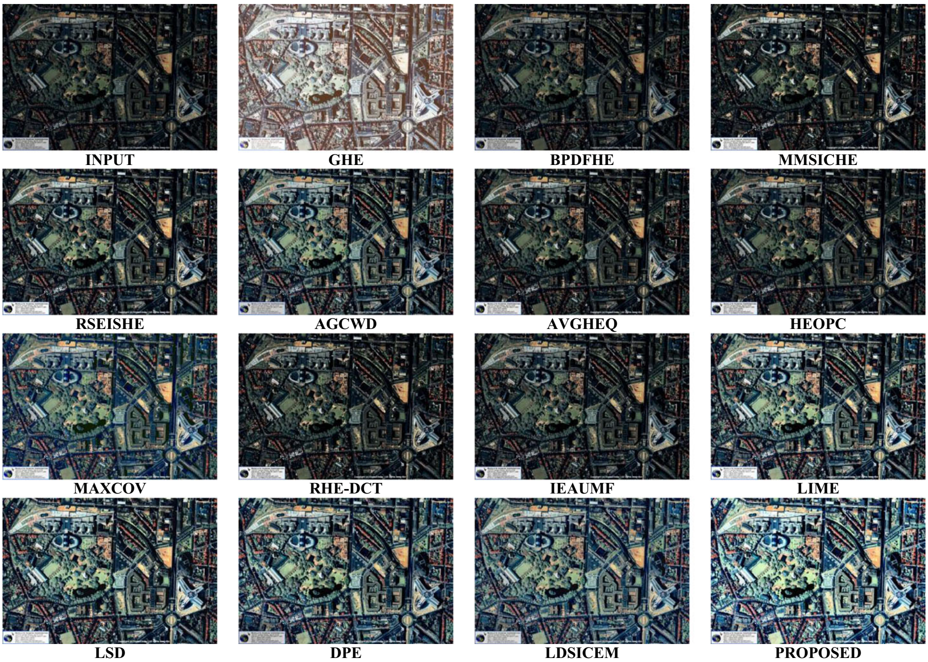

Fig. 12 Quality enhanced results of different algorithms for "Image 10"

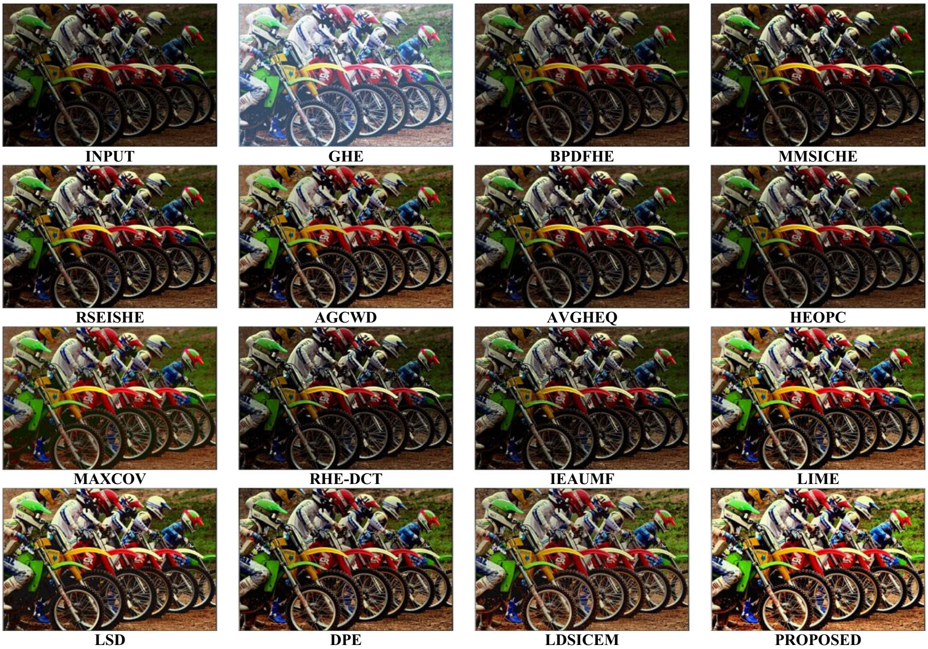

Fig. 13 Quality enhanced results of different algorithms for "Image 11"

GLCM-homogeneity (*GH*) can be characterized by the closeness of neighboring pixels with reference pixels. Intuitively, these are also responsible for uniformity of texture, and hence, expressed as:

$$GH = -\sum_{m=0}^{M-1}\sum_{n=0}^{N-1}\Psi(m,n)log_2\Psi(m,n), \tag{23}$$

Qualitative (visual) analysis for enhancement of images is shown in Figs. 3, 4, 5, 6, 7, 8, 9, 10, 11, 12, 13, 14, 15, 16, 17, 18, 19, 20, 21 and 23. Comparative evaluation for Brightness (B), Contrast (V), Entropy (E), Sharpness (S), colourfulness (C), GLCM-homogeneity (GH), GLCM-energy (GE), GLCM-correlation (GC) are listed in Tables 2 to 9, respectively. It can be easily noticed from the tabular results that both entropy and contrast are highly desirable along with image sharpness content of the information. Also, certain amount of brightness should be also increased, which is also desired for clear contrast evaluation in case of dark images.

Also, for identifying the textural improvement, GLCM based performance measures like GLCM- are also employed and the excellence of the proposed model, and the lower value are desired for GLCM-homogeneity, GLCM-energy, GLCM-correlation for better visualization in context of both human as well as machine-vision perspective.

Finally, it can be easily concluded that this approach outperforms the other state-of-the-art approaches. The novelty of the work can be justified as the re-allocation of intensity levels for corresponding pixel elements is so precise due to least successive differential change in PSNR value which ensures that further division or further reconstruction is obviously redundant. As this statistical moment-based redistribution needs only 2–4 iterations at most for subsequent histogram division, otherwise this approach is free from iterative greedy algorithms and hence system complexity is not

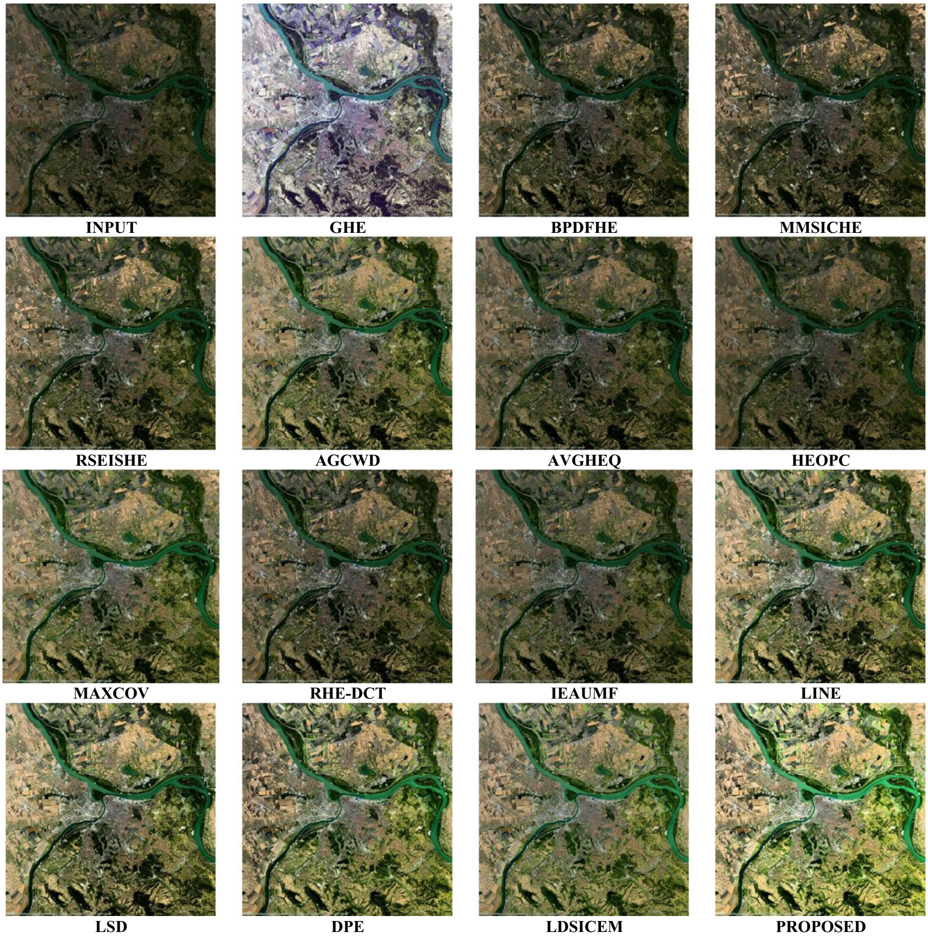

Fig. 14 Quality enhanced results of different algorithms for "Image 12"

so high. Due to this adaptive behavior of the intensity distribution the gamma value-set when derived from it, is obviously highly adaptive and here individual gamma values those evaluated explicitly raised over reconstructed intensity values, unlike conventional gamma correction methods. Unlike greedy algorithms, it is a parameter-free approach, hence no pre-specified count for sub-divisions. It imparts the better gamma-corrected intensity distribution throughout the dynamic range. In addition multiple repetitive equalizations like other methods have been avoided for extreme intensity levels according to the image behavior. Here, only the in-between middle range ($\mu_1 - \sigma_1, \mu_1 + \sigma_1$) is only operated for further sub-division (which is also limited to 2–3 iterations) the range and rest of the intensity values themselves decide their adaptive gamma value-set locally. This is the sole region that over-enhancement (which leads to saturated patches) and under-enhancement (which leads to dark patches) can be easily avoided and hence, naturally looking, quality enhanced images can be achieved. Desired time-complexity analysis is also presented in Table 10 and Fig. 22, by executing the proposed method as well as all the state-of-the-art methodologies in a similar environment. The running time is calculated as an averaged execution time for a set of 120 test images.

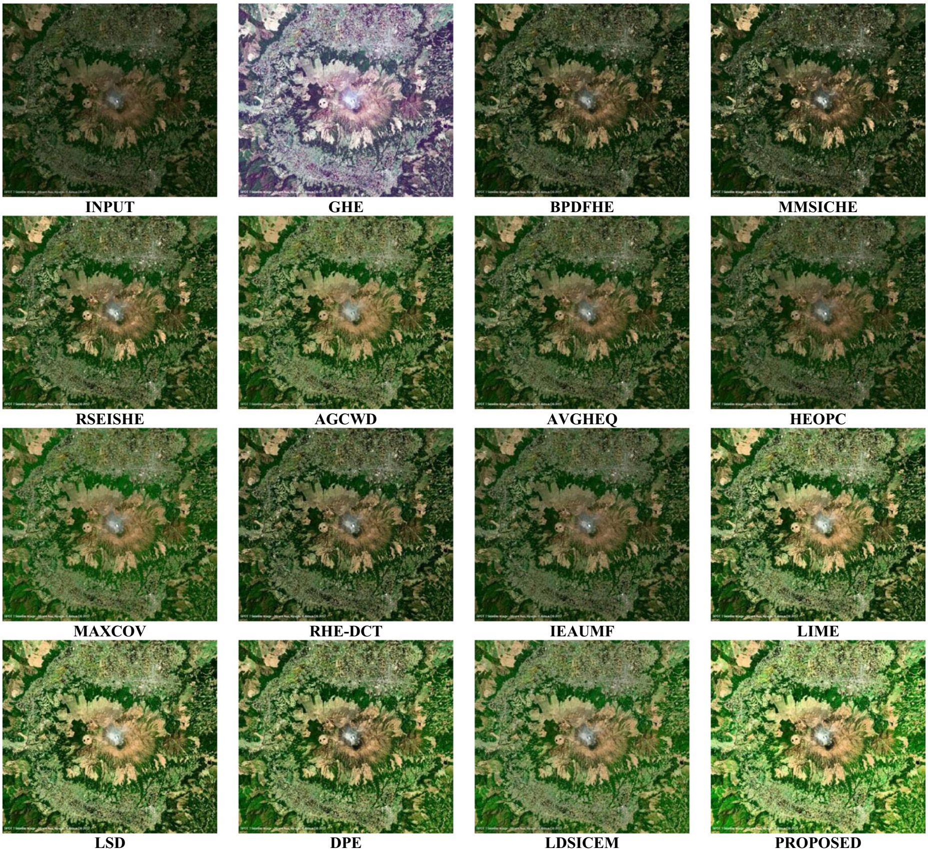

Fig. 15 Quality enhanced results of different algorithms for "Image 13"

4 Conclusion

In this paper, a new quality enhancement approach especially for dark or poorly illuminated images with a core objective to re-allocate the processed pixels using reclusive histogram sub-division along with an adaptive stopping criterion based on pixel wise relative L_2-norm basis (which itself is intuitively related to optimal PSNR value). Employing such kind information preserved signal reconstruction based stopping criterion makes the desired intensity distribution easy achievable in less iterations and hence complexity hike due iterative behaviour can be easily compensated to a great extent. Hence, iteration count only ranges from 2 to 3. Perfectly reconstructed, moment-centered piecewise sub-equalized statistical distribution which intuitively leads to the adaptive or image dependent evaluation of the desired gamma value-set, so that precise re-allocation of the transformed intensity bin-values. Due to this adaptive behavior of the intensity distribution the gamma value-set when derived from it, is obviously highly adaptive and here individual gamma values are evaluated explicitly raised over reconstructed intensity values, unlike conventional gamma correction methods. This adaptiveness makes the entire methodology highly capable for covering a wide variety of images, due to which robustness of the algorithm also increases. The proposed methodology has been verified on various dark images. The desired performance has been achieved visually and also measured by using relevant image quality matrices.

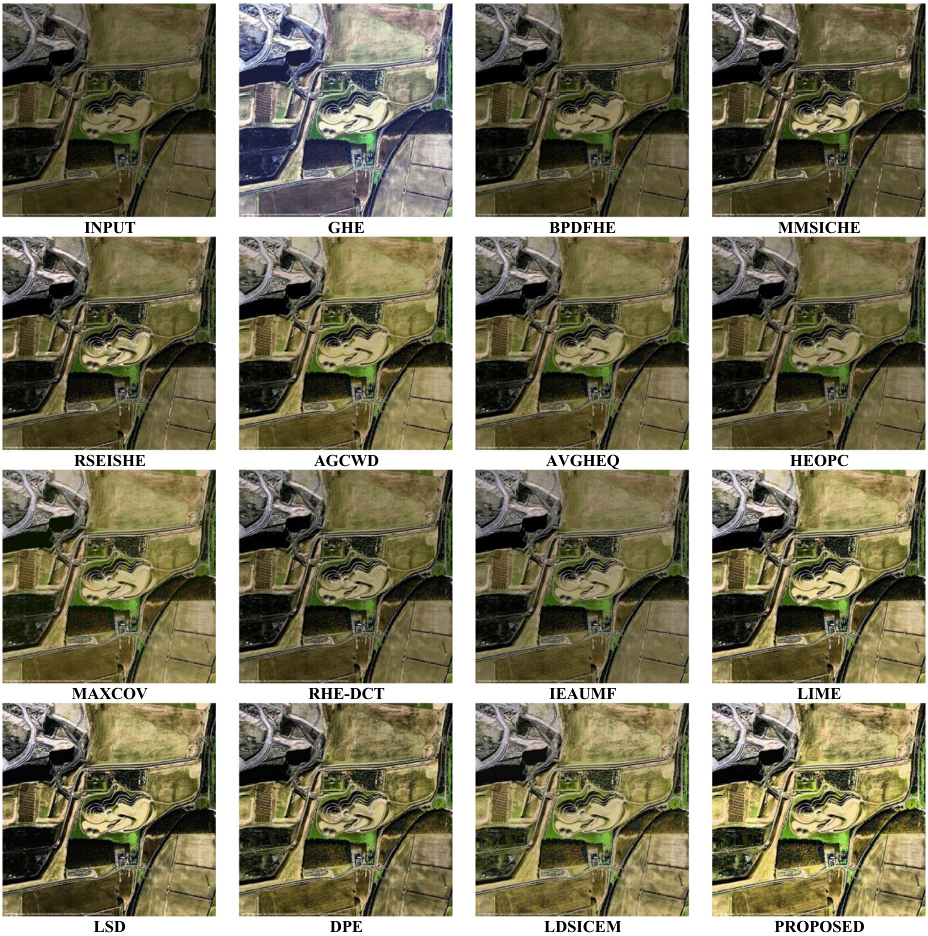

Fig. 16 Quality enhanced results of different algorithms for "Image 14"

Fig. 17 Quality enhanced results of different algorithms for "Image 15"

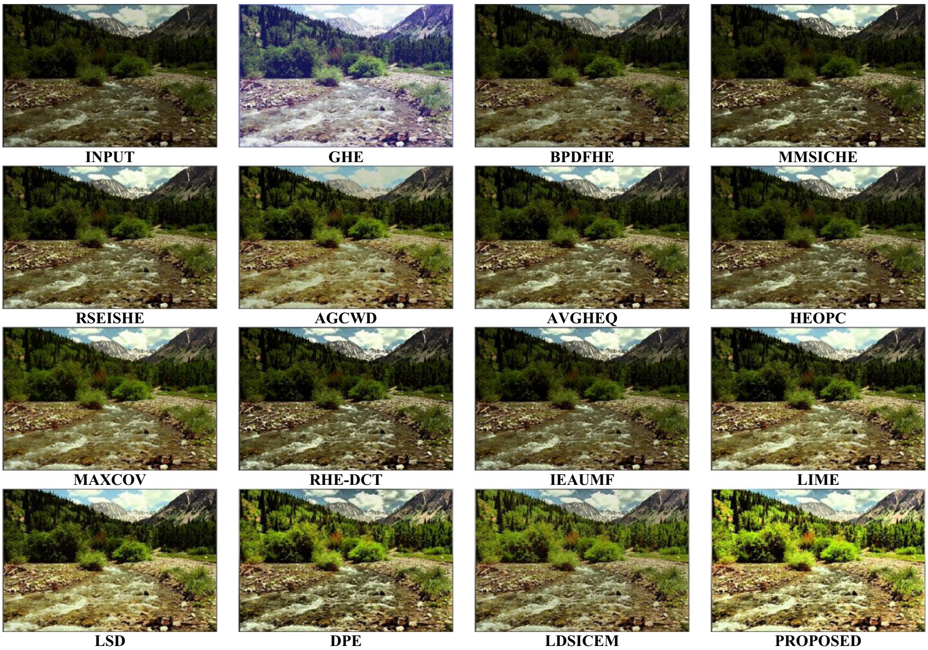

Fig. 18 Quality enhanced results of different algorithms for "Image 16"

Fig. 19 Quality enhanced results of different algorithms for "Image 17"

Fig. 20 Quality enhanced results of different algorithms for "Image 18"

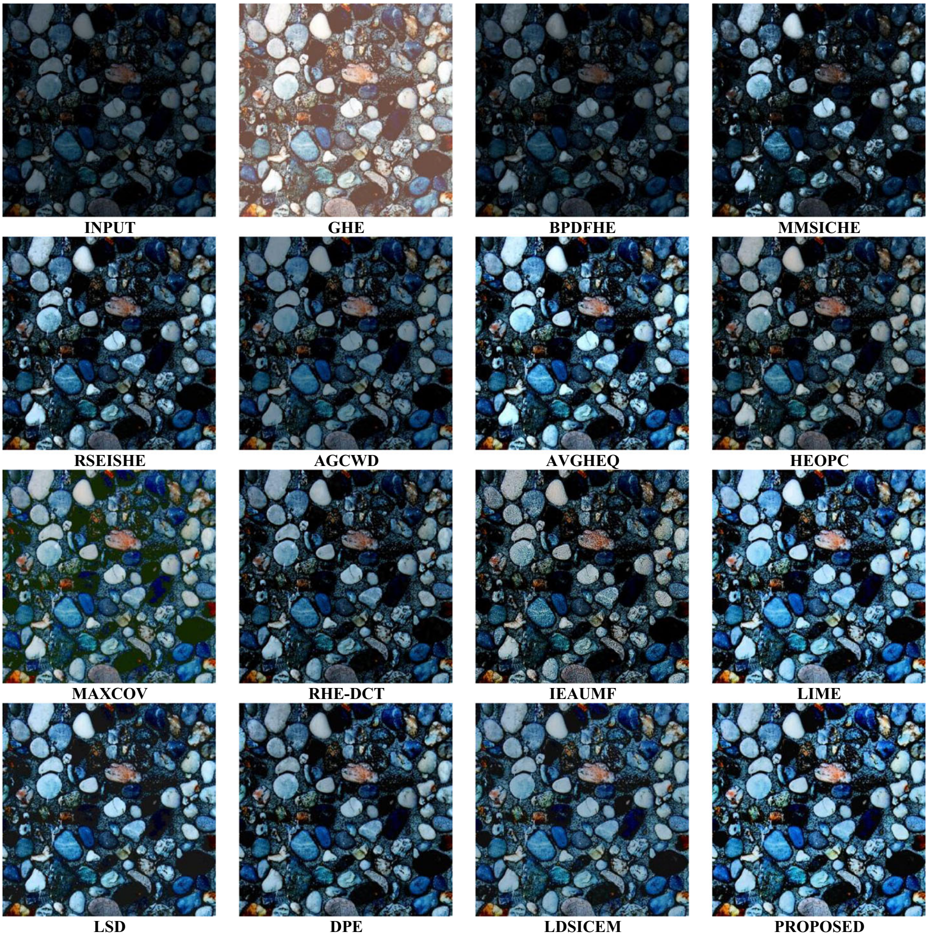

Fig. 21 Quality enhanced results of different algorithms for "Image 19"

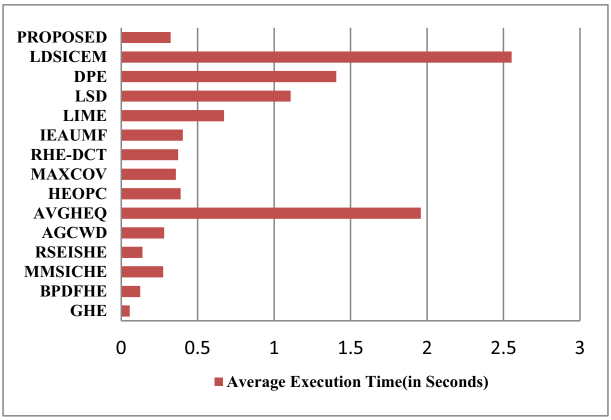

Fig. 22 Comparative analysis for execution times

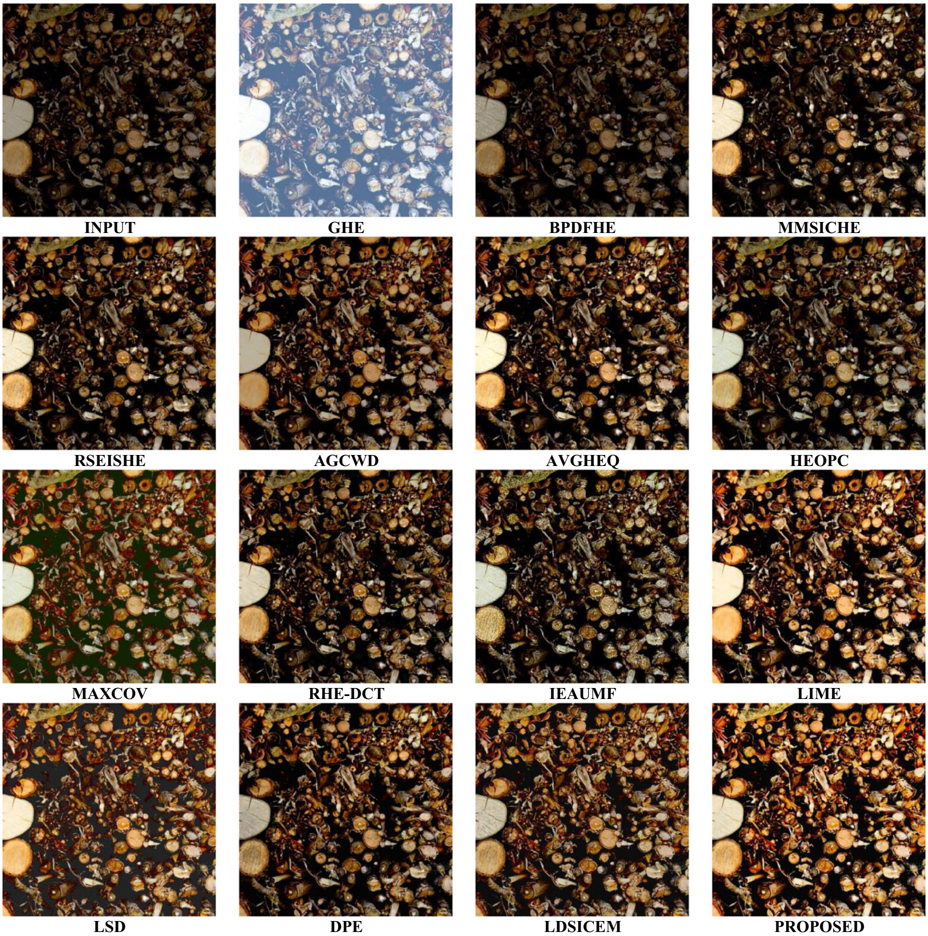

Fig. 23 Quality enhanced results of different algorithms for "Image 20"

Table 10 Average execution time (in seconds) for comparative quantitative evaluation among various algorithms

METHOD	GHE	BPDFHE	MMSICHE	RSEISHE	AGCWD
TIME (in Seconds)	0.057	0.124	0.275	0.139	0.282
METHOD	AVGHEQ	HEOPC	MAXCOV	RHE-DCT	IEAUMF
TIME (in Seconds)	1.959	0.389	0.358	0.373	0.404
METHOD	LIME	LSD	DPE	LDSICEM	PROPOSED
TIME (in Seconds)	0.673	1.109	1.407	2.553	0.324

References

1. Cai J, Gu S, Zhang L (2018) Learning a deep single image contrast enhancer from multi-exposure images. IEEE Trans Image Process 27(4):2049–2062
2. Chen C, Chen Q, Xu J, Koltun V (2018) Learning to see in the dark. In IEEE Conference on Computer Vision and Pattern Recognition, pp. 3291–3300
3. Chen YS, Wang YC, Kao MH, Chuang YY (2018) Deep photo enhancer: unpaired learning for image enhancement from photographs with gans. In IEEE/CVF Conference on Computer Vision and Pattern Recognition, pp 6306–6314
4. Fu X, Wang J, Zeng D, Huang Y, Ding X (2015) Remote sensing image enhancement using regularized-histogram equalization and DCT. IEEE Geosci Remote Sens Lett 12(11):2301–2305
5. Gonzalez RC, Woods RE (2017) Digital image processing, 4th edn. Pearson/Prentice-Hall, New York
6. Guo X, Li Y, Ling H (2017) LIME: Low-light image enhancement via illumination map estimation. IEEE Trans Image Process 26(2):982–993
7. Huang SC, Cheng FC, Chiu YS (2013) Efficient Contrast Enhancement Using Adaptive Gamma Correction with Weighting Distribution. IEEE Trans Image Process 22(3):1032–1041
8. Huang SC, Yeh CH (2013) Image contrast enhancement for preserving mean brightness without losing image features. Journal of Engg Applications of Artificial Intelligence 26(5):1487–1492
9. Kodak Lossless True Color Image Suite. http://r0k.us/graphics/kodak/. Accessed 02 June 2017
10. Lin SCF, Wong CY, Jiang G, Rahman MA, Ren TR, Kwok N, Shi H, Yu YH, Wu T (2016) Intensity and edge based adaptive unsharp masking filter for color image enhancement. Optik–Int J Light Electron Optics 127(1):407–414
11. Lin SCF, Wong CY, Rahman MA, Jiang G, Liu S, Kwok N, Shi H, Yu YH, Wu T (2015) Image enhancement using the averaging histogram equalization (AVHEQ) approach for contrast improvement and brightness Preservation. Comput Electr 46:356–370
12. NASA Visible Earth. https://visibleearth.nasa.gov. Accessed 02 June 2017
13. Pléiades Satellite Image. https://intelligence-airbusds.com. Accessed 02 June 2017
14. Satellite Imagery and Geospatial Services | SATPALDA. https://satpalda.com. Accessed 02 June 2017
15. Sheet D, Garud H, Suveer A, Mahadevappa M, Chatterjee J (2010) Brightness preserving dynamic fuzzy histogram equalization. IEEE Trans Consum Electron 56(4):2475–2480
16. Singh H, Agrawal N, Kumar A, Singh GK, & Lee HN (2016) A novel gamma correction approach using optimally clipped sub-equalization for dark image enhancement. 21 IEEE International Conference on Digital Signal Processing (DSP), Beijing, pp 497–501. https://doi.org/10.1109/ICDSP.2016.7868607
17. Singh K, Kapoor R (2014) Image enhancement using exposure based sub image histogram equalization. Pattern Recogn Lett 36:10–14
18. Singh K, Kapoor R (2014) Image enhancement via median-mean based sub-image-clipped histogram equalization. Optik -Int J Light Electron Optics 125(17):4646–4651
19. Singh K, Kapoor R, Sinha SK (2015) Enhancement of low exposure images via recursive histogram equalization algorithms. Optik 126:2619–2625
20. Singh H, Kumar A (2016) Satellite image enhancement using beta wavelet based gamma corrected adaptive knee transformation. 5th IEEE International Conference on Communication and Signal Processing (ICCSP), Melmaruvathur, pp 128–132
21. Singh H, Kumar A, Balyan LK, Singh GK (2018) Swarm intelligence optimized piecewise gamma corrected histogram equalization for dark image enhancement. Comput Electr Eng 70:462–475
22. Singh, H., Kumar, A., & Balyan, L. K. (2017). Cuckoo search optimizer based piecewise gamma corrected auto-clipped tile-wise equalization for satellite image enhancement. In 14th IEEE India Council International Conference (INDICON), Roorkee, India, 2017, pp 1–6. https://doi.org/10.1109/INDICON.2017.8487901
23. Singh H, Kumar A, Balyan LK (2017) A levy flight firefly optimizer based piecewise gamma corrected unsharp masking framework for satellite image enhancement. In 14th IEEE India Council International Conference (INDICON), Roorkee, India, 2017, pp 1–5. https://doi.org/10.1109/INDICON.2017.8487501
24. Singh H, Kumar A, Balyan LK, Singh GK (2017) A novel optimally weighted framework of piecewise gamma corrected fractional order masking for satellite image enhancement. Computers and Electrical Engineering, (in press): 1–17. https://doi.org/10.1016/j.compeleceng.2017.11.014
25. Singh H, Kumar A, Balyan LK, Singh GK (2017) A novel optimally gamma corrected intensity span maximization approach for dark image enhancement. In 22nd IEEE. International Conference on Digital Signal Processing (DSP) 2017 (pp. 1–5). https://doi.org/10.1109/ICDSP.2017.8096035
26. Singh H, Kumar A, Balyan LK Lee HN (2018) Piecewise gamma corrected optimally framed Grumwald-Letnikov fractional differential masking for satellite image enhancement. In 7th IEEE International

Conference on Communication and Signal Processing (ICCSP), Chennai, India, 2018, pp 0129–0133. https://doi.org/10.1109/ICCSP.2018.8524564
27. Singh H, Kumar A, Balyan LK, Lee HN (2018) Fuzzified histogram equalization based gamma corrected cosine transformed energy redistribution for image enhancement. In 23rd IEEE International Conference on Digital Signal Processing (DSP), Shanghai, China, 2018, pp 1–5. https://doi.org/10.1109/ICDSP.2018.8631612
28. Singh H, Kumar A, Balyan LK, Singh GK (2018) Slantlet filter-bank-based satellite image enhancement using gamma-corrected knee transformation. Int J Electron 105(10):1695–1715. https://doi.org/10.1080/00207217.2018.1477199
29. Singh H, Kumar A, Balyan LK (2019) A sine-cosine optimizer-based gamma corrected adaptive fractional differential masking for satellite image enhancement. In Harmony Search and Nature Inspired Optimization Algorithms. Advances in Intelligent Systems and Computing, vol 741, pp 633–645 Springer, Singapore. https://doi.org/10.1007/978-981-13-0761-4_61.
30. Wong CY, Jiang G, Rahman MA, Liu S, Lin SCF, Kwok N, Shi H, Yu YH, Wu T (2016) Histogram equalization and optimal profile compression based approach for colour image enhancement. J Visual Commun and Image Represen 38:802–813
31. Wong CY, Liu S, Liu SC, Rahman MA, Lin SCF, Jiang G, Kwok N, Shi H (2016) Image contrast enhancement using histogram equalization with maximum intensity coverage. J Mod Opt 63(16):1618–1629

Himanshu Singh received the B. E. (Hons.) in Electronics and Communication Engineering from MITS Gwalior, India in 2010. He is currently pursuing Ph.D. (Dual Degree) in Electronics and Communication Engineering at Indian Institute of Information Technology Design and Manufacturing (IIITDM) Jabalpur, India. His research interests include satellite image enhancement, image segmentation, image denoising, image compression and optimization techniques.

Anil Kumar is an assistant professor in discipline of Electronics and Communication Engineering IIITDM, Jabalpur, India. He did his B.E. from Army Institute of Technology, Pune, India in Electronics and Telecommunication Engineering, and M.Tech. and Ph.D. from IIT Roorkee, India in 2002, 2006 and 2010, respectively. His research interests include Digital Filters, Multirate Filter Bank Designing, Signal and Image Processing.

L. K. Balyan is an assistant professor of mathematics in the discipline of Natural Science at IIITDM, Jabalpur. He did his Master of Science in applied mathematics from Indian Institute of Technology (IIT), Roorkee and Ph.D in applied mathematics from IIT Kanpur in 2009. His research interests include numerical solution of partial differential equations and spectral methods and their applications.

H. N. Lee received the B.S., M.S., and Ph.D. degrees from the University of California, Los Angeles, CA, USA, in 1993, 1994, and 1999, respectively, all in electrical engineering. He was with the HRL Laboratories, LLC, Malibu, CA, USA, as a Research Staff Member from 1999 to 2002. From 2002 to 2008, he was an Assistant Professor with the University of Pittsburgh, PA, USA. In 2009, he then moved to the School of Electrical Engineering and Computer Science, Gwangju Institute of Science and Technology, South Korea, where he is currently affiliated. His areas of research include information theory, signal processing theory, communications/networking theory, and their application to wireless communications and networking, compressive sensing, future internet, and brain–computer interface.

Affiliations

Himanshu Singh[1] · **Anil Kumar**[1] · **L. K. Balyan**[1] · **H. N. Lee**[2]

[1] Indian Institute of Information Technology, Design and Manufacturing Jabalpur, Jabalpur, India

[2] Gwangju Institute of Science and Technology, Gwangju, South Korea